# Prediction of the unit cell edge length of cubic $A_2^{2+}BB'O_6$ perovskites by multiple linear regression and artificial neural networks

Sandra Dimitrovska*, Slobotka Aleksovska, Igor Kuzmanovski†

*Institute of Chemistry, Faculty of Natural Sciences and Mathematics
University "Sv. Kiril i Metodij",
PO Box 162, 1001 Skopje, Republic of Macedonia*

**Abstract:** The unit cell edge length, $a$, of a set of complex cubic perovskites having the general formula $A_2^{2+}BB'O_6$ is predicted using two methodologies: multiple linear regression and artificial neural networks. The unit cell edge length is expressed as a function of six independent variables: the effective ionic radii of the constituents (A, B and B′), the electronegativities of B and B′, and the oxidation state of B. In this analysis, 147 perovskites of the $A_2^{2+}BB'O_6$ type, having the cubic structure and belonging to the $Fm3m$ space group, are included. They are divided in two sets; 98 compounds are used in the calibration set and 49 are used in the test set. Both models give consistent results and could be successfully used to predict the lattice cell parameter of new members of this series.

*Keywords: complex perovskites, lattice parameters, artificial neural networks, multiple linear regression*

## 1 Introduction

Recently, investigations of compounds with the perovskite structure have attracted great interest because of their useful physical and chemical properties [1–3]. As a result, many compounds that belong in this group have been synthesized. Now, not only simple $ABO_3$ compounds are included under the name perovskite but also different series of compounds containing mixed cations, for example: $(A'_xA''_{1-x})BO_3$, $A(B'_xB''_{1-x})O_3$, $(A'_{1-x}A''_x)BO_3$, $(A'_xA''_{1-x})(B'_xB''_{1-x})O_3$.

---

* E-mail: sandra@iunona.pmf.ukim.edu.mk
† E-mail: shigor@iunona.pmf.ukim.edu.mk

Historically, the original perovskite ($CaTiO_3$) was identified as crystallizing in the cubic space group, *Pm3m* [1]. Further investigation revealed a distortion from cubic structure, lowering the symmetry of $CaTiO_3$ from cubic to orthorhombic [4]. The nature of distortion most likely depends upon the size of the ionic radii of the O-anion and A, B cations. Refinement of the crystal structures of different perovskite compounds reveals the existence of different crystal systems (orthorhombic, rombohedral, monoclinic, etc [1–3]).

The large number of compounds reported, and the possibility of synthesizing of new perovskite compounds underscores the usefulness of the ability to predict their structure and properties. Therefore, numerous attempts have been made to correlate structural parameters with physical variables of the constituent elements [5–10].

In our previous work, linear regression was used to predict the cell parameters and the complete crystal structures of another series of compounds [11–16]. Recently, we predicted unit cell parameters of orthorhombic perovskites by multiple linear regression and artificial neural networks [17]. Continuing our work on perovskite compounds, we have concentrated on complex perovskites with the general formula $A_2^{2+}BB'O_6$. These perovskites with multiple B-cation sites form one of the largest groups of complex perovskites and adopt different crystal structures [1–3]. The largest isomorphous subgroup of this type of complex perovskites belongs to the cubic space group, *Fm3m*. In this structure, the two different cations B and B', are alternatively distributed in equivalent crystallographic positions (Fig. 1). The oxidation state of B cations may vary, however, so the compounds are of several types as: $A_2^{2+}B^{1+}B'^{7+}O_6$, $A_2^{2+}B^{2+}B'^{6+}O_6$, $A_2^{2+}B^{3+}B'^{5+}O_6$. If the difference in the valence and the radii between B and B' are both large, the compounds adopt an ordered cubic structure [1]. However, there are some more subtle electronic factors that are responsible for order/disordered cubic structures [8].



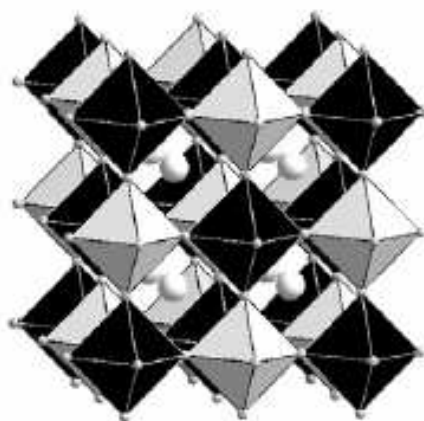**Fig. 1** Crystal structure of an ordered double perovskite with general formula $A_2BB'O_6$.

Continuing our work in the field of perovskites, and on structural correlations of isomorphous/isostructural series, we present a simple model for predicting the length of unit cell edge of cubic perovskites with general formula $A_2BB'O_6$ by two methods:

multiple linear regression (MLR) and artificial neural networks (ANN).

## 2   Data analysis

### 2.1   Choice of the sample and the independent variables

The lattice parameter of the cubic $A_2BB'O_6$ type perovskites was taken to be the dependent variable in the analysis. The lengths of the unit cell edge $(a/\text{Å})$ for 147 perovskites of $A_2BB'O_6$ type, with an $(NH_4)_3FeF_6$ structure and $Fm3m$ space group, were retrieved from the literature [1, 18–33]. In order to make comparisons between the two models, the data were divided randomly into two subsets: the calibration subset with 98 compounds and test subset with 49 compounds.

First, three independent variables are considered, namely the effective ionic radii of the constituents. The values of the effective ionic radii for the corresponding oxidation states and coordination numbers are taken from Shannon [34]. Thus, the cations in A-position were treated as twelve-coordinate, and the cations in B-position as six-coordinate in their high spin state.

In this isomorphous series, the B-cations are in different oxidation states, another independent variable was included in the analysis. The sum of the oxidation states for cations in the B-position is eight, thus, only the oxidation state $(z)$ of one of the B-cations is an independent variable, e.g. of the B-cation in lower oxidation state. The analysis shows that this independent variable is statistically significant.

Another factor affecting the crystal structure might be the electronegativity $(x)$ of the constituents, taking into account that the difference between the electronegativity of the cations and the anion (oxygen) affects the degree of the ionic character of the bond. With few exceptions, $Ba^{2+}$, $Sr^{2+}$ and $Ca^{2+}$ are the cations found in the A-position; the electronegativity of the cations in the A-position is not statistically significant. However, the electronegativities of the B-cations were statistically significant and were included in the analysis. The values for Pauling's electronegativities are found in reference [35].

The input data (for both the independent and the dependent variables) for the calibration set are given in Table 1.

### 2.2   Modeling

Two methods of analysis were used in this work: multiple linear regression (MLR) and artificial neural networks (ANN). Both were chosen because of their powerful predictive abilities.

The MLR was performed using the program package STATGRAPHICS PLUS Ver. 3.0 [36]. The length of the unit cell edge, $a$, was expressed as a function of six independent variables:

$$a/\text{Å} = b + c \cdot r(A)/\text{Å} + d \cdot r(B)/\text{Å} + e \cdot r(B')/\text{Å} + f \cdot x(B) + g \cdot x(B') + h \cdot z(B) \quad (1)$$

The symbols of the dependent and independent variables in the previous equation are given in the text above. The parameter $b$ is the intercept of the regression surface, and $c$, $d$, $e$, $f$, $g$ and $h$ are the slopes of the regression surface with respect to each variable. As the variables are dimensionless (the unit cell length and the radii of the constituents are divided by Å), the parameters are dimensionless, as well.

In recent years, ANNs have proven to be useful algorithms, and they have been applied to solve different chemical problems [37,38]. Their theoretical basis is well documented in the chemometric literature [38], so only the procedure for their optimization will be described here.

In this study we used three layered, feed-forward neural networks with six input neurons (determined by the number of independent variables), one output neuron (determined by the number of dependent variables) with a linear transfer function [38] and one hidden layer with neurons having a sigmoid transfer function [38]. The optimal network architecture was searched by changing the number of neurons in the hidden layer from one to ten. The Nguyen-Widrow [39] algorithm was used for initialization of the weights and biases for the networks. The networks were optimized using the Levenberg-Marquardt algorithm [40] for the back-propagation of error and implemented in the programming package Matlab [41].

The generalization abilities of the ANNs were controlled by an early stopping procedure. For this purpose, we had to divide the calibration set into two subsets (a training set and a validation set) consisting of 49 samples. The training set serves to optimize the weights and biases of the ANNs, and each network architecture was trained forty times. The validation set serves to monitor the performance of the ANNs during the training. If an error in the validation set starts to increase during the training, the network starts to overfit the data. If this is repeated in ten consecutive training cycles, the training is stopped, and the weights and biases corresponding to a minimal error in the validation set are restored. Although this technique could be criticized, because it requires the division of the available samples into two subsets for training, it does give good results [17, 42–43].

## 3   Results and discussion

The estimated coefficients of the proposed MLR model developed using the calibration set, as well as the standard errors and $t$-statistics (Table 1) are given in Table 2.

The adjusted coefficient of determination $R^2_{adj}$. for the developed model is 96.92 %, which means that the regression equation can successfully predict the unit cell length of other members in the series. The predicted values of the unit cell length compared with the actual values for the compounds in calibration set are given in Table 3. There is an excellent agreement between the actual and predicted values, except for four of them. The largest discrepancy appears for $Ca_2CaWO_6$. However, the calculated tolerance factor (0.88) for this compound is at the lower limit for these structures (0.87-1.04).

The performance of the model developed was verified using an independent set of variables (test set) consisting of 49 perovskite samples, which were not used during the

calibration. The predicted and the actual values of unit cell parameter for the compounds in the test set, as well as, the absolute errors are presented in Table 4.

The root mean square error of prediction ($RMSEP$) was calculated in order to estimate the performances of the model:

$$RMSEP = \sqrt{\frac{\sum_i (a_{i,\text{ actual}} - a_{i,\text{ predicted}})^2}{i}} \qquad (2)$$

In equation (2), $i$ is the number of samples in the test set, $a_{i,\text{ actual}}$ is the experimental value of the unit cell parameter for the sample $i$, and $a_{i,\text{ predicted}}$ is the predicted value for the same sample. The calculated $RMSEP$ for the model developed by MLR is 0.0552 Å.

Among different network architectures, the one with two neurons in the hidden layer shows the best predictive ability. The $RMSEP$ for the network with the best prediction ability (among those with two neurons in the hidden layer) is 0.0497 Å.

The results obtained by ANN are also presented in Table 4. There is excellent agreement between the actual (experimentally obtained) and the predicted values of the unit cell length obtained by each model. The values obtained for the residuals by both methods are comparable. Thus, in both cases there are just three values which exceed 0.100 Å for the same compounds, and one additional value obtained only by ANN. The mean absolute error obtained by MLR is 0.042 Å and 0.037 Å by ANN.

In order to gain even better insight into the predictive power of the proposed models (MLR and ANN), graphs correlating the actual and predicted values for the unit cell edge length for the compounds in the test set are given in Fig 2.
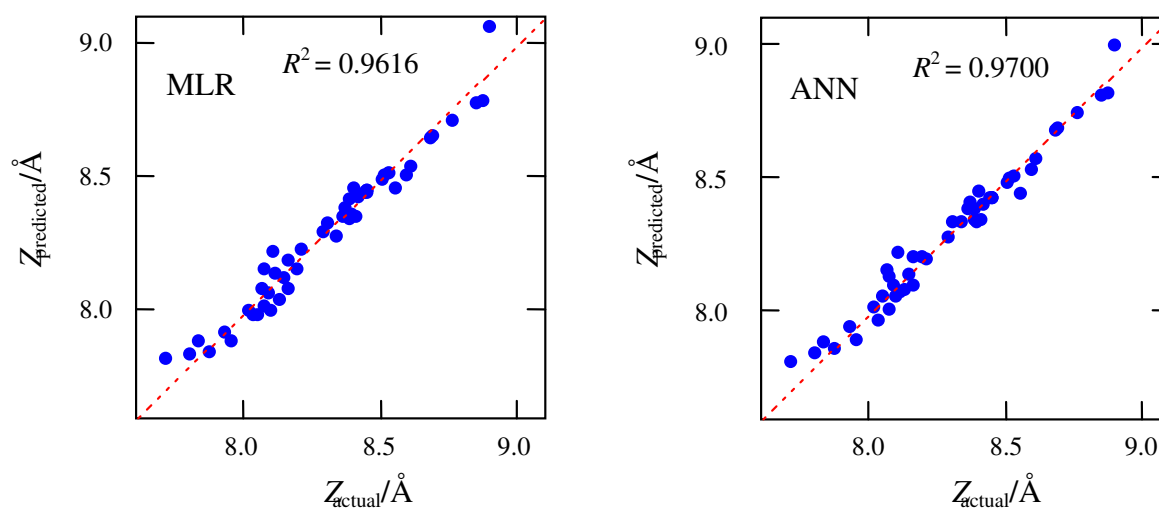


**Fig. 2** Correlation between actual and predicted values for $a$ by MLR and ANN.

Since the $RMSEP$ obtained using the ANN model was found to be smaller than the one corresponding to the MLR model, we applied the $F$-test in order to determine if the difference in $RMSEP$ was statistically significant:

$$F(n_1, n_2) = RMSEP_{\text{MLR}}^2 / RMSEP_{\text{ANN}}^2 \qquad (3)$$

where $n_1$ and $n_2$ are the number of samples in the test set used in the MLR and ANN models, respectively. At a level of significance of 0.95 the calculated $F$ value (1.250) is lower that the critical one (1.615), indicating that there is no statistical difference in *RMSEP* values predicted by MLR and feed-forward neural networks.

## 4　Conclusion

The length of the unit cell edge of cubic complex perovskites of the general formula $A_2BB'O_6$ are successfully expressed as a function of six independent variables (the effective ionic radii of the constituents, the electronegativities of B-ions, and the oxidation state of the B' cation). Here, we have compared two simple models (MLR and ANN) for the prediction of the unit cell parameters. Both models give excellent results and therefore, could be used to predict the unit cell parameters of new members of this series. Although the ANNs are capable of modeling possible nonlinearities among independent and dependent variables, in this case there is no statistically significant difference between the predictions of the two models.

## References

[1] F.S. Galasso (Ed.): *Structure, Properties and Preparation of Perovskite-type Compounds,* Pergamon Press, Oxford, 1969 (and references therein).

[2] E.J. Baran: "Structural chemistry and physicochemical properties of perovskite-like Materials", *Catalysis Today,* Vol. 8, (1990), pp. 133–151 (and the references therein).

[3] P.W. Barnes: *Exploring structural changes and distortions in quaternary perovskites and defect pyrochlores using powder diffraction techniques,* Thesis(PhD), The Ohio State University, 2003.

[4] R.H. Butner and E.N. Maslen: "Electron difference density and structural parameters in $CaTiO_3$", *Acta Cryst. B,* Vol. 48, (1992), pp. 644–649.

[5] O. Fukunaga and T. Fujita: "The relationship between ionic radii and cell volumes in the perovskite compounds", *J. Solid State Chem.,* Vol. 8, (1973), pp. 331–338.

[6] D.M. Giaquinta and H. Conrad zur Loye: "Structural predictions in the $ABO_3$ phase diagram", *Chem. Mater.,* Vol. 6, (1994), pp. 365–372.

[7] N.W. Thomas: "A new global parameterization of perovskite structures", *Acta Cryst. B,* Vol. 54, (1998), pp. 585–594.

[8] A.A. Bokov, N.P. Protsenko and Z.-G. Ye: "Relationship between ionicity, ionic radii and order/disorder in complex perovskites", *J. Phys. Chem. Solids*, Vol. 61, (2000), pp. 1519–1527.

[9] M.W. Lufaso and P.M. Woodward: "Prediction of the crystal structure of perovskites using the software program SpuDS", *Acta Cryst. B,* Vol. 57, (2001), pp. 725–738.

[10] L. Chonghe, T. Yihao, Z. Yingzhi, W. Chunmei and W. Ping: "Prediction of lattice constants in perovskites of $GdFeO_3$ structure", *J. Phys. Chem. Solids,* Vol. 64, (2003), pp. 2147–2156.

[11] V. Petruševski and S. Aleksovska: "Correlations between effective crystal radii and unit cell volume in Tutton salts", *Croat. Chem. Acta,* Vol. 64(4), (1991), pp. 577–583.

[12] V. Petruševski and S. Aleksovska: "Structural correlations in alums", *Croat. Chem. Acta,* Vol. 67, (1994), pp. 221–230.

[13] S. Aleksovska, V. Petruševski and Lj. Pejov: "Crystal structures of members in isostructural series: prediction of the crystal structure of $Cs_2MnO_4$ – a $\beta$-$K_2SO_4$ type isomorph", *Croat. Chem. Acta,* Vol. 70, (1997), pp. 1009–1019.

[14] S. Aleksovska, S.C. Nyburg, Lj. Pejov and V.M. Petruševski: "$\beta$-$K_2SO_4$ type isomorphs: prediction of structure and refinement of $Rb_2CrO_4$", *Acta Cryst. B,* Vol. 54, (1998), pp. 115–120.

[15] S. Aleksovska, V.M. Petruševski and B. Šoptrajanov: "Calculation of structural parameters in isostructural series: the kieserite group", *Acta Cryst. B,* Vol. 54, (1998), pp. 564–567.

[16] V.M. Petruševski and S. Aleksovska: "Dependence of the crystal structure parameters on the size of the structural units in some isomorphous/isostructural series", *Croat. Chem. Acta,* Vol. 72(1), (1999), pp. 71–76.

[17] I. Kuzmanovski and S. Aleksovska: "Optimization of artificial neural networks for prediction of the unit cell parameters in orthorhombic perovskites. Comparison with multiple linear regression", *Chemometr. Intell. Lab. Syst.,* Vol. 67, (2003), pp. 167–174.

[18] K.E. Stitzer, M.D. Smith and H.-C. zur Loye: "Crystal growth of $Ba_2MOsO_6$ (M = Li, Na) from reactive hydroxy fluxes", *Solid State Sciences,* Vol. 4, (2002), pp. 311–316.

[19] Y. Izumiyama, Y. Doi, M. Wakeshima, Y. Hinatsu, A. Nakamura and Y. Ishii: "Magnetic and calorimetric studies on ordered perovskite $Ba_2ErRuO_6$", *J. Solid State Chem.,* Vol. 169(1), (2002), pp. 125–130.

[20] S.B. Kim, B.W. Lee and C.S. Kim: "Neutron and Mössbauer studies of the double perovskite $A_2FeMoO_6$ (A=Sr and Ba)", *J. Magn. and Magn. Mater.* Vol. 242-245, (2002), pp. 747–750.

[21] J.B. Philipp, P. Majewski, L. Alff, A. Erb, R. Gross, T. Graf, M.S. Brandt, J. Simon, T. Walther, W. Mader, D. Topwal and D.D. Sarma: "Structural and doping effects in the half metallic double perovskite $A_2CrWO_6$", *Phys. Rev. B,* Vol. 68, (2003), pp. 144431–144445.

[22] W.T. Fu and D.J.W. Ijdo: "On the Structure of $BaTl_{0.5}Sb_{0.5}O_3$: An Ordered Perovskite", *J. Solid State Chem.* Vol. 128, (1997), pp. 323–325.

[23] W. Dmowski, M.K. Akbas, P.K. Davies and T. Egami: "Local structure of $Pb(Sc_{1/2}Ta_{1/2})O_3$ and related structures", *J. Phys. Chem. Solids,* Vol. 61, (2000), pp. 229–237.

[24] D.-Y. Jung, G. Demazeau and J.-H. Chof: "Iridium(III) stabilized in oxygen lattices of perovskite structure $Sr_2MIr^{III}O_6$ (M = Nb, Ta)", *J. Mater. Chem.,* Vol. 5(3), (1995), pp. 517–519.

[25] P.E. Kazin, A.M. Abakumov, D.D. Zaytsev, Yu.D. Tretyakov, N.R. Khasanova, G. Van Tendeloo and M. Jansen: "Synthesis and crystal structure of $Sr_2ScBiO_6$", *J. Solid State Chem.,* Vol. 162(1), (2001), pp. 142–147.

[26] H.W. Eng: *The crystal and electronic structures of oxides containing $d^0$ transition metals in octahedral coordination,* Thesis (PhD), The Ohio State University, 2003.

[27] Y. Teraoka, M.-D. Wei and S. Kagawa: "Double perovskites containing hexavalent molybdenum and tungsten: synthesis, structural investigation and proposal of fitness factor to discriminate the crystal symmetry", *J. Mater. Chem.,* Vol. 8(11), (1998), pp. 2323–2325.

[28] M.J. Martínez-Lope, J.A. Alonso, M.T. Casais and M.T. Fernández-Díaz: "Preparation, crystal and magnetic structure of the double perovskites $Ba_2CoBO_6$ (B = Mo, W)", *Europian J. Inorg. Chem.,* Vol. 2002(9), (2002), pp. 2463–2469.

[29] A.K. Azad, S.-G. Eriksson, S.A. Ivanov, R. Mathieu, P. Svedlindh, J. Eriksen and H. Rundlöf: "Synthesis, structural and magnetic characterisation of the double perovskite $A_2MnMoO_6$ (A=Ba, Sr)", *J. Alloys and Comp.,* Vol. 364(1-2), (2004), pp. 77–82.

[30] C.M. Lapa, Y.P. Yadava, R.A. Sanguinetti Ferreira, J. Albino Aguiar, C.L. Da Silva, D.P.F. De Souza: "Production, sintering and microstructural characteristics of $Ba_2NiWO_6$ complex perovskite oxide ceramics", *Acta Microscopica,* Vol. 12 Supplement C, (2003) (XIX Congress of the Brazilian Society for Microscopy and Microanalysis), pp. 77–78.

[31] S.-O. Lee, T.Y. Cho and S.-H. Byeon: "Magnetic propertiy of oxide with the perovskite structure, $A_2Fe(III)BO_6$ (A=Ca, Sr, Ba and B=Sb, Bi)", *Bull. Korean Chem. Soc,* Vol. 18(1), (1997), pp. 91–97.

[32] G. Baldinozzi, Ph. Sciau, M. Pinot and D. Grebille: "Crystal structure of the antiferroelectric perovskite $Pb_2MgWO_6$", *Acta Cryst. B,* Vol. 51, (1995), pp. 668–673.

[33] V. Primo-Martín and M. Jansen: "Synthesis, Structure, and Physical Properties of Cobalt Perovskites: $Sr_3CoSb_2O_9$ and $Sr_2CoSbO_{6-\delta}$", *J. Solid State Chem.,* Vol. 157, (2001), pp. 76–85.

[34] R.D. Shannon: "Revised effective ionic radii in halides and chalcogenides" *Acta Cryst. A,* Vol. 32, (1976), pp. 751–767.

[35] D.R. Lide: *Handbook of Chemistry and Physics,* CRC Press/Chapman and Hall, Boca Raton, FL/London, 2002.

[36] *STATGRAPHICS PLUS*, VER. 3.0, Statistical Graphics Package, Educational Institution edition, Statistical Graphics, 1994–1997.

[37] A. Bos, M. Bos and W.E. van der Linden: "Artificial neural networks as a tool for soft-modelling in quantitative analytical chemistry: the prediction of the water content of cheese", *Anal. Chim. Acta*, Vol. 256, (1992), pp. 133–144.

[38] J. Zupan and J. Gasteiger: *Neural Networks in Chemistry and Drug Design*, WCH, Weinhaim, 1999.

[39] D. Nguyen and B. Widrow: "Inproving the learning speed of 2- layer neural network by choosing initial values of the asaptive weights", *IEEE Proc. 1st Int. Joint Conf. Neural Networks*, Vol. 3, (1990), pp. 21–26.

[40] J.J. Moré: "The Levenberg-Marquardt Algorithm: Implementation and Theory", In: G.A. Watson (Ed.): *Numerical Analysis*, Lecture Notes in Mathematics 630, Springer Verlag, 1977, pp. 105–116.

[41] *MATLAB 6.0*, Mathworks, 1984–2000.

[42] I. Kuzmanovski, M. Trpkovska, B. Šoptrajanov and V. Stefov: "Determination of the composition of human urinary calculi composed of whewellite, weddellite and

carbonate apatite using artificial neural networks", *Anal. Chim. Acta*, Vol. 491, (2003), pp. 211–218.

[43] I. Kuzmanovski, M. Ristova, B. Šoptrajanov, V. Stefov and V. Popovski: "Determination of the composition of sialoliths composed of carbonate apatite and albumin using artificial neural networks", *Talanta,* Vol. 62, (2004), pp. 813–817.

|     | Formula | $r(A)/\text{Å}$ | $r(B)/\text{Å}$ | $r(B')/\text{Å}$ | $x(B)$ | $x(B')$ | $z(B)$ | $a/\text{Å}$ | Ref. |
|-----|---------|---------|---------|----------|--------|---------|--------|--------|------|
|     | Calibration set | | | | | | | | |
| 1   | $Ba_2AgIO_6$ | 1.61 | 1.15 | 0.53 | 1.93 | 2.66 | 1 | 8.46 | [1] |
| 2   | $Ba_2LiOsO_6$ | 1.61 | 0.76 | 0.525 | 0.98 | 2.2 | 1 | 8.1046 | [18] |
| 3   | $Ba_2NaIO_6$ | 1.61 | 1.02 | 0.53 | 0.93 | 2.66 | 1 | 8.33 | [1] |
| 4   | $Ba_2NaOsO_6$ | 1.61 | 1.02 | 0.525 | 0.93 | 2.2 | 1 | 8.287 | [18] |
| 5   | $Ca_2LiOsO_6$ | 1.34 | 0.76 | 0.525 | 0.98 | 2.2 | 1 | 7.83 | [1] |
| 6   | $Ca_2LiReO_6$ | 1.34 | 0.76 | 0.53 | 0.98 | 1.9 | 1 | 7.83 | [1] |
| 7   | $Sr_2LiReO_6$ | 1.44 | 0.76 | 0.53 | 0.98 | 1.9 | 1 | 7.87 | [1] |
| 8   | $Sr_2NaOsO_6$ | 1.44 | 1.02 | 0.525 | 0.93 | 2.2 | 1 | 8.13 | [1] |
| 9   | $Ba_2BiTaO_6$ | 1.61 | 1.03 | 0.64 | 1.9 | 1.5 | 3 | 8.568 | [1] |
| 10  | $Ba_2CePaO_6$ | 1.61 | 1.01 | 0.78 | 1.12 | 1.5 | 3 | 8.8 | [1] |
| 11  | $Ba_2DyNbO_6$ | 1.61 | 0.912 | 0.64 | 1.22 | 1.6 | 3 | 8.437 | [1] |
| 12  | $Ba_2DyPaO_6$ | 1.61 | 0.912 | 0.78 | 1.22 | 1.5 | 3 | 8.74 | [1] |
| 13  | $Ba_2ErNbO_6$ | 1.61 | 0.89 | 0.64 | 1.24 | 1.6 | 3 | 8.427 | [1] |
| 14  | $Ba_2ErPaO_6$ | 1.61 | 0.89 | 0.78 | 1.24 | 1.5 | 3 | 8.716 | [1] |
| 15  | $Ba_2ErRuO_6$ | 1.61 | 0.89 | 0.565 | 1.24 | 2.2 | 3 | 8.323 | [19] |
| 16  | $Ba_2ErTaO_6$ | 1.61 | 0.89 | 0.64 | 1.24 | 1.5 | 3 | 8.423 | [1] |
| 17  | $Ba_2EuNbO_6$ | 1.61 | 0.947 | 0.64 | 1.12 | 1.6 | 3 | 8.507 | [1] |
| 18  | $Ba_2EuPaO_6$ | 1.61 | 0.947 | 0.78 | 1.12 | 1.5 | 3 | 8.783 | [1] |
| 19  | $Ba_2FeMoO_6$ | 1.61 | 0.645 | 0.61 | 1.83 | 2.16 | 3 | 8.0747 | [20] |
| 20  | $Ba_2FeReO_6$ | 1.61 | 0.645 | 0.58 | 1.83 | 1.9 | 3 | 8.05 | [1] |
| 21  | $Ba_2GdPaO_6$ | 1.61 | 0.938 | 0.78 | 1.2 | 1.5 | 3 | 8.774 | [1] |
| 22  | $Ba_2GdReO_6$ | 1.61 | 0.938 | 0.58 | 1.2 | 1.9 | 3 | 8.431 | [1] |
| 23  | $Ba_2HoNbO_6$ | 1.61 | 0.901 | 0.64 | 1.23 | 1.6 | 3 | 8.434 | [1] |
| 24  | $Ba_2HoPaO_6$ | 1.61 | 0.901 | 0.78 | 1.23 | 1.5 | 3 | 8.73 | [1] |
| 25  | $Ba_2InNbO_6$ | 1.61 | 0.8 | 0.64 | 1.78 | 1.6 | 3 | 8.279 | [1] |
| 26  | $Ba_2InOsO_6$ | 1.61 | 0.8 | 0.575 | 1.78 | 2.2 | 3 | 8.224 | [1] |
| 27  | $Ba_2InReO_6$ | 1.61 | 0.8 | 0.58 | 1.78 | 1.9 | 3 | 8.258 | [1] |
| 28  | $Ba_2InSbO_6$ | 1.61 | 0.8 | 0.6 | 1.78 | 2.05 | 3 | 8.269 | [1] |
| 29  | $Ba_2InUO_6$ | 1.61 | 0.8 | 0.76 | 1.78 | 1.7 | 3 | 8.52 | [1] |
| 30  | $Ba_2LaPaO_6$ | 1.61 | 1.032 | 0.78 | 1.1 | 1.5 | 3 | 8.885 | [1] |
| 31  | $Ba_2LuNbO_6$ | 1.61 | 0.861 | 0.64 | 1 | 1.6 | 3 | 8.364 | [1] |
| 32  | $Ba_2LuPaO_6$ | 1.61 | 0.861 | 0.78 | 1 | 1.5 | 3 | 8.666 | [1] |
| 33  | $Ba_2MnReO_6$ | 1.61 | 0.645 | 0.58 | 1.55 | 1.9 | 3 | 8.18 | [21] |
| 34  | $Ba_2NdNbO_6$ | 1.61 | 0.983 | 0.64 | 1.14 | 1.6 | 3 | 8.54 | [1] |
| 35  | $Ba_2NdReO_6$ | 1.61 | 0.983 | 0.58 | 1.14 | 1.9 | 3 | 8.51 | [1] |
| 36  | $Ba_2NdTaO_6$ | 1.61 | 0.983 | 0.64 | 1.14 | 1.5 | 3 | 8.556 | [1] |

*Some literature data [33] refer this compound as rhombohedral;
**The value for the pseudocubic unit cell parameter was taken.

**Table 1** Input data in the analysis: radii of the constituents ($r$), electronegativity of the B-cations ($x$), the oxidation state of B-cation ($z$) and lattice parameter ($a$).

| | Formula | $r(A)/\text{Å}$ | $r(B)/\text{Å}$ | $r(B')/\text{Å}$ | $x(B)$ | $x(B')$ | $z(B)$ | $a/\text{Å}$ | Ref. |
|---|---|---|---|---|---|---|---|---|---|
| 37 | $Ba_2RhNbO_6$ | 1.61 | 0.745 | 0.64 | 2.28 | 1.6 | 3 | 8.17 | [1] |
| 38 | $Ba_2ScNbO_6$ | 1.61 | 0.745 | 0.64 | 1.36 | 1.6 | 3 | 8.23402 | [3] |
| 39 | $Ba_2ScPaO_6$ | 1.61 | 0.745 | 0.78 | 1.36 | 1.5 | 3 | 8.549 | [1] |
| 40 | $Ba_2ScReO_6$ | 1.61 | 0.745 | 0.58 | 1.36 | 1.9 | 3 | 8.163 | [1] |
| 41 | $Ba_2ScTaO_6$ | 1.61 | 0.745 | 0.64 | 1.36 | 1.5 | 3 | 8.23147 | [3] |
| 42 | $Ba_2ScUO_6$ | 1.61 | 0.745 | 0.76 | 1.36 | 1.7 | 3 | 8.49 | [1] |
| 43 | $Ba_2SmPaO_6$ | 1.61 | 0.958 | 0.78 | 1.17 | 1.5 | 3 | 8.792 | [1] |
| 44 | $Ba_2SmTaO_6$ | 1.61 | 0.958 | 0.64 | 1.17 | 1.5 | 3 | 8.519 | [1] |
| 45 | $Ba_2TlSbO_6$ | 1.61 | 0.885 | 0.6 | 1.8 | 2.05 | 3 | 8.3809 | [22] |
| 46 | $Ba_2TlTaO_6$ | 1.61 | 0.885 | 0.64 | 1.8 | 1.5 | 3 | 8.42 | [1] |
| 47 | $Ba_2TmPaO_6$ | 1.61 | 0.88 | 0.78 | 1.25 | 1.5 | 3 | 8.692 | [1] |
| 48 | $Ba_2TmTaO_6$ | 1.61 | 0.88 | 0.64 | 1.25 | 1.5 | 3 | 8.406 | [1] |
| 49 | $Ba_2YPaO_6$ | 1.61 | 0.9 | 0.78 | 1.22 | 1.5 | 3 | 8.718 | [1] |
| 50 | $Ba_2YReO_6$ | 1.61 | 0.9 | 0.58 | 1.22 | 1.9 | 3 | 8.372 | [1] |
| 51 | $Ba_2YUO_6$ | 1.61 | 0.9 | 0.76 | 1.22 | 1.7 | 3 | 8.69 | [1] |
| 52 | $Ba_2YbNbO_6$ | 1.61 | 0.868 | 0.64 | 1.21 | 1.6 | 3 | 8.374 | [1] |
| 53 | $Ba_2YbTaO_6$ | 1.61 | 0.868 | 0.64 | 1.21 | 1.5 | 3 | 8.39 | [1] |
| 54 | $Pb_2ScTaO_6$ | 1.49 | 0.745 | 0.64 | 1.36 | 1.5 | 3 | 8.1401 | [23] |
| 55 | $Sr_2AlTaO_6$ | 1.44 | 0.535 | 0.64 | 1.61 | 1.5 | 3 | 7.79133 | [3] |
| 56 | $Sr_2CoSbO_6^*$ | 1.44 | 0.61 | 0.6 | 1.88 | 2.05 | 3 | 7.88 | [24] |
| 57 | $Sr_2CrOsO_6$ | 1.44 | 0.615 | 0.575 | 1.66 | 2.2 | 3 | 7.84 | [1] |
| 58 | $Sr_2CrWO_6$ | 1.44 | 0.615 | 0.62 | 1.66 | 1.7 | 3 | 7.82 | [21] |
| 59 | $Sr_2GaOsO_6$ | 1.44 | 0.62 | 0.575 | 1.81 | 2.2 | 3 | 7.82 | [1] |
| 60 | $Sr_2GaReO_6$ | 1.44 | 0.62 | 0.58 | 1.81 | 1.9 | 3 | 7.843 | [1] |
| 61 | $Sr_2InReO_6$ | 1.44 | 0.8 | 0.58 | 1.78 | 1.9 | 3 | 8.071 | [1] |
| 62 | $Sr_2InUO_6$ | 1.44 | 0.8 | 0.76 | 1.78 | 1.7 | 3 | 8.33 | [1] |
| 63 | $Sr_2ScBiO_6^{**}$ | 1.44 | 0.745 | 0.76 | 1.36 | 1.9 | 3 | 8.1816 | [25] |
| 64 | $Sr_2ScOsO_6$ | 1.44 | 0.745 | 0.575 | 1.36 | 2.2 | 3 | 8.02 | [1] |
| 65 | $Sr_2RhTaO_6$ | 1.44 | 0.665 | 0.64 | 2.28 | 1.5 | 3 | 7.939 | [24] |
| 66 | $Sr_2CrNbO_6$ | 1.44 | 0.615 | 0.64 | 1.66 | 1.6 | 3 | 7.87 | [1] |
| 67 | $Ba_2CaMoO_6$ | 1.61 | 1 | 0.59 | 1 | 2.16 | 2 | 8.3803 | [26] |
| 68 | $Ba_2CaOsO_6$ | 1.61 | 1 | 0.545 | 1 | 2.2 | 2 | 8.362 | [1] |
| 69 | $Ba_2CaTeO_6$ | 1.61 | 1 | 0.56 | 1 | 2.1 | 2 | 8.393 | [1] |
| 70 | $Ba_2CaUO_6$ | 1.61 | 1 | 0.73 | 1 | 1.7 | 2 | 8.67 | [1] |
| 71 | $Ba_2CdMoO_6$ | 1.61 | 0.95 | 0.59 | 1.69 | 2.16 | 2 | 8.3242 | [27] |
| 72 | $Ba_2CdOsO_6$ | 1.61 | 0.95 | 0.545 | 1.69 | 2.2 | 2 | 8.325 | [1] |
| 73 | $Ba_2CoMoO_6$ | 1.61 | 0.745 | 0.59 | 1.88 | 2.16 | 2 | 8.08623 | [28] |
| 74 | $Ba_2CoReO_6$ | 1.61 | 0.745 | 0.55 | 1.88 | 1.9 | 2 | 8.086 | [1] |
| 75 | $Ba_2CoWO_6$ | 1.61 | 0.745 | 0.6 | 1.88 | 1.7 | 2 | 8.10799 | [28] |

**Table 1** (continue) Input data in the analysis: radii of the constituents ($r$), electronegativity of the B-cations ($x$), the oxidation state of B-cation ($z$) and lattice parameter ($a$).

| | Formula | $r(A)/\text{Å}$ | $r(B)/\text{Å}$ | $r(B')/\text{Å}$ | $x(B)$ | $x(B')$ | $z(B)$ | $a/\text{Å}$ | Ref. |
|---|---|---|---|---|---|---|---|---|---|
| 76 | $Ba_2CrUO_6$ | 1.61 | 0.8 | 0.73 | 1.66 | 1.7 | 2 | 8.297 | [1] |
| 77 | $Ba_2FeUO_6$ | 1.61 | 0.78 | 0.73 | 1.83 | 1.7 | 2 | 8.312 | [1] |
| 78 | $Ba_2MgMoO_6$ | 1.61 | 0.72 | 0.59 | 1.31 | 2.16 | 2 | 8.08377 | [26] |
| 79 | $Ba_2MgReO_6$ | 1.61 | 0.72 | 0.55 | 1.31 | 1.9 | 2 | 8.082 | [1] |
| 80 | $Ba_2MgTeO_6$ | 1.61 | 0.72 | 0.56 | 1.31 | 2.1 | 2 | 8.13 | [1] |
| 81 | $Ba_2MgWO_6$ | 1.61 | 0.72 | 0.6 | 1.31 | 1.7 | 2 | 8.09849 | [26] |
| 82 | $Ba_2MnMoO_6$ | 1.61 | 0.83 | 0.59 | 1.55 | 2.16 | 2 | 8.168 | [29] |
| 83 | $Ba_2MnUO_6$ | 1.61 | 0.83 | 0.73 | 1.55 | 1.7 | 2 | 8.52 | [1] |
| 84 | $Ba_2NiMoO_6$ | 1.61 | 0.69 | 0.59 | 1.91 | 2.16 | 2 | 8.035 | [27] |
| 85 | $Ba_2NiUO_6$ | 1.61 | 0.69 | 0.73 | 1.91 | 1.7 | 2 | 8.336 | [1] |
| 86 | $Ba_2NiWO_6$ | 1.61 | 0.69 | 0.6 | 1.91 | 1.7 | 2 | 8.0748 | [30] |
| 87 | $Ba_2ZnOsO_6$ | 1.61 | 0.74 | 0.545 | 1.65 | 2.2 | 2 | 8.095 | [1] |
| 88 | $Ba_2ZnReO_6$ | 1.61 | 0.74 | 0.55 | 1.65 | 1.9 | 2 | 8.106 | [1] |
| 89 | $Ba_2ZnWO_6$ | 1.61 | 0.74 | 0.6 | 1.65 | 1.7 | 2 | 8.11612 | [26] |
| 90 | $Ca_2CaWO_6$ | 1.34 | 1 | 0.6 | 1 | 1.7 | 2 | 8 | [1] |
| 91 | $Pb_2FeWO_6$ | 1.49 | 0.78 | 0.6 | 1.83 | 1.7 | 2 | 8.05 | [1] |
| 92 | $Pb_2MgTeO_6$ | 1.49 | 0.72 | 0.56 | 1.31 | 2.1 | 2 | 7.99 | [1] |
| 93 | $Sr_2CaOsO_6$ | 1.44 | 1 | 0.545 | 1 | 2.2 | 2 | 8.21 | [1] |
| 94 | $Sr_2CoUO_6$ | 1.44 | 0.745 | 0.73 | 1.88 | 1.7 | 2 | 8.19 | [1] |
| 95 | $Sr_2FeOsO_6$ | 1.44 | 0.78 | 0.545 | 1.83 | 2.2 | 2 | 7.85 | [1] |
| 96 | $Sr_2FeUO_6$ | 1.44 | 0.78 | 0.73 | 1.83 | 1.7 | 2 | 8.11 | [1] |
| 97 | $Sr_2MgUO_6$ | 1.44 | 0.72 | 0.73 | 1.31 | 1.7 | 2 | 8.19 | [1] |
| 98 | $Sr_2MnUO_6$ | 1.44 | 0.83 | 0.73 | 1.55 | 1.7 | 2 | 8.28 | [1] |

**Table 1** (continue) Input data in the analysis: radii of the constituents ($r$), electronegativity of the B-cations ($x$), the oxidation state of B-cation ($z$) and lattice parameter ($a$).

| Coefficient | Numerical value | Standard error | $t$-statistic |
|:---:|:---:|:---:|:---:|
| $b$ | 4.3966 | 0.1302 | 33.775 |
| $c$ | 1.1659 | 0.0662 | 17.602 |
| $d$ | 1.0637 | 0.0493 | 21.565 |
| $e$ | 1.7085 | 0.0843 | 20.265 |
| $f$ | -0.0747 | 0.0170 | -4.3942 |
| $g$ | 0.0435 | 0.0259 | 1.6770 |
| $h$ | 0.0499 | 0.0094 | 5.3276 |

**Table 2** Numerical values of coefficients estimated by MLR, standard errors and $t-$statistics.

| Formula | $a(\text{act.})/\text{Å}$ | $a(\text{pred.})/\text{Å}$ | $|\Delta a|/\text{Å}$ |
|---|---|---|---|
| $Ba_2AgIO_6$ | 8.46 | 8.424 | 0.036 |
| $Ba_2LiOsO_6$ | 8.1046 | 8.052 | 0.053 |
| $Ba_2NaIO_6$ | 8.33 | 8.361 | -0.031 |
| $Ba_2NaOsO_6$ | 8.287 | 8.332 | -0.045 |
| $Ca_2LiOsO_6$ | 7.83 | 7.737 | 0.093 |
| $Ca_2LiReO_6$ | 7.83 | 7.732 | 0.098 |
| $Sr_2LiReO_6$ | 7.87 | 7.849 | 0.021 |
| $Sr_2NaOsO_6$ | 8.13 | 8.134 | -0.004 |
| $Ba_2BiTaO_6$ | 8.568 | 8.536 | 0.032 |
| $Ba_2CePaO_6$ | 8.8 | 8.812 | -0.012 |
| $Ba_2DyNbO_6$ | 8.437 | 8.466 | -0.029 |
| $Ba_2DyPaO_6$ | 8.74 | 8.701 | 0.039 |
| $Ba_2ErNbO_6$ | 8.427 | 8.441 | -0.014 |
| $Ba_2ErPaO_6$ | 8.716 | 8.676 | 0.040 |
| $Ba_2ErRuO_6$ | 8.323 | 8.339 | -0.016 |
| $Ba_2ErTaO_6$ | 8.423 | 8.436 | -0.013 |
| $Ba_2EuNbO_6$ | 8.507 | 8.510 | -0.003 |
| $Ba_2EuPaO_6$ | 8.783 | 8.745 | 0.038 |
| $Ba_2FeMoO_6$ | 8.0747 | 8.109 | -0.034 |
| $Ba_2FeReO_6$ | 8.05 | 8.047 | 0.003 |
| $Ba_2GdPaO_6$ | 8.774 | 8.730 | 0.044 |
| $Ba_2GdReO_6$ | 8.431 | 8.405 | 0.026 |
| $Ba_2HoNbO_6$ | 8.434 | 8.453 | -0.019 |
| $Ba_2HoPaO_6$ | 8.73 | 8.688 | 0.042 |
| $Ba_2InNbO_6$ | 8.279 | 8.305 | -0.026 |
| $Ba_2InOsO_6$ | 8.224 | 8.220 | 0.004 |
| $Ba_2InReO_6$ | 8.258 | 8.215 | 0.043 |
| $Ba_2InSbO_6$ | 8.269 | 8.256 | 0.013 |
| $Ba_2InUO_6$ | 8.52 | 8.514 | 0.006 |
| $Ba_2LaPaO_6$ | 8.885 | 8.837 | 0.048 |
| $Ba_2LuNbO_6$ | 8.364 | 8.428 | -0.064 |
| $Ba_2LuPaO_6$ | 8.666 | 8.663 | 0.003 |
| $Ba_2MnReO_6$ | 8.18 | 8.213 | 0.033 |
| $Ba_2NdNbO_6$ | 8.54 | 8.547 | -0.007 |
| $Ba_2NdReO_6$ | 8.51 | 8.458 | 0.052 |
| $Ba_2NdTaO_6$ | 8.556 | 8.543 | 0.013 |
| $Ba_2RhNbO_6$ | 8.17 | 8.209 | -0.039 |
| $Ba_2ScNbO_6$ | 8.23402 | 8.278 | -0.044 |

**Table 3** Actual, predicted values for the unit cell length, as well as, absolute errors for the compounds of the calibration set obtained by MLR.

| Formula | $a$(act.)/Å | $a$(pred.)/Å | $|\Delta a|$/Å |
|---|---|---|---|
| $Ba_2ScPaO_6$ | 8.549 | 8.512 | 0.037 |
| $Ba_2ScReO_6$ | 8.163 | 8.188 | -0.025 |
| $Ba_2ScTaO_6$ | 8.23147 | 8.273 | -0.042 |
| $Ba_2ScUO_6$ | 8.49 | 8.487 | 0.003 |
| $Ba_2SmPaO_6$ | 8.792 | 8.753 | 0.039 |
| $Ba_2SmTaO_6$ | 8.519 | 8.514 | 0.005 |
| $Ba_2TlSbO_6$ | 8.3809 | 8.345 | 0.036 |
| $Ba_2TlTaO_6$ | 8.42 | 8.389 | 0.031 |
| $Ba_2TmPaO_6$ | 8.692 | 8.664 | 0.028 |
| $Ba_2TmTaO_6$ | 8.406 | 8.425 | -0.019 |
| $Ba_2YPaO_6$ | 8.718 | 8.688 | 0.030 |
| $Ba_2YReO_6$ | 8.372 | 8.363 | 0.009 |
| $Ba_2YUO_6$ | 8.69 | 8.662 | 0.028 |
| $Ba_2YbNbO_6$ | 8.374 | 8.420 | -0.046 |
| $Ba_2YbTaO_6$ | 8.39 | 8.415 | -0.025 |
| $Pb_2ScTaO_6$ | 8.1401 | 8.133 | 0.007 |
| $Sr_2AlTaO_6$ | 7.79133 | 7.833 | -0.042 |
| $Sr_2CoSbO_6$ | 7.88 | 7.848 | 0.032 |
| $Sr_2CrOsO_6$ | 7.84 | 7.834 | 0.006 |
| $Sr_2CrWO_6$ | 7.82 | 7.889 | -0.069 |
| $Sr_2GaOsO_6$ | 7.82 | 7.828 | -0.008 |
| $Sr_2GaReO_6$ | 7.843 | 7.823 | 0.020 |
| $Sr_2InReO_6$ | 8.071 | 8.017 | 0.054 |
| $Sr_2InUO_6$ | 8.33 | 8.316 | 0.014 |
| $Sr_2ScBiO_6$ | 8.1816 | 8.297 | -0.116 |
| $Sr_2ScOsO_6$ | 8.02 | 7.994 | 0.026 |
| $Sr_2RhTaO_6$ | 7.939 | 7.921 | 0.018 |
| $Sr_2CrNbO_6$ | 7.87 | 7.919 | -0.049 |
| $Ba_2CaMoO_6$ | 8.3803 | 8.465 | -0.084 |
| $Ba_2CaOsO_6$ | 8.362 | 8.390 | -0.028 |
| $Ba_2CaTeO_6$ | 8.393 | 8.411 | -0.018 |
| $Ba_2CaUO_6$ | 8.67 | 8.684 | -0.014 |
| $Ba_2CdMoO_6$ | 8.3242 | 8.360 | -0.036 |
| $Ba_2CdOsO_6$ | 8.325 | 8.285 | 0.040 |
| $Ba_2CoMoO_6$ | 8.08623 | 8.128 | -0.041 |
| $Ba_2CoReO_6$ | 8.086 | 8.048 | 0.038 |
| $Ba_2CoWO_6$ | 8.10799 | 8.125 | -0.017 |
| $Ba_2CrUO_6$ | 8.297 | 8.422 | -0.125 |
| $Ba_2FeUO_6$ | 8.312 | 8.388 | -0.076 |

**Table 3** (continue) Actual, predicted values for the unit cell length, as well as, absolute errors for the compounds of the calibration set obtained by MLR.

| Formula | $a$(act.)/Å | $a$(pred.)/Å | $|\Delta a|$/Å |
|---------|-------------|--------------|----------------|
| $Ba_2MgMoO_6$ | 8.08377 | 8.144 | -0.060 |
| $Ba_2MgReO_6$ | 8.082 | 8.064 | 0.018 |
| $Ba_2MgTeO_6$ | 8.13 | 8.090 | 0.040 |
| $Ba_2MgWO_6$ | 8.09849 | 8.141 | -0.042 |
| $Ba_2MnMoO_6$ | 8.168 | 8.243 | -0.075 |
| $Ba_2MnUO_6$ | 8.52 | 8.462 | 0.058 |
| $Ba_2NiMoO_6$ | 8.035 | 8.067 | -0.032 |
| $Ba_2NiUO_6$ | 8.336 | 8.286 | 0.050 |
| $Ba_2NiWO_6$ | 8.0748 | 8.064 | 0.011 |
| $Ba_2ZnOsO_6$ | 8.095 | 8.064 | 0.031 |
| $Ba_2ZnReO_6$ | 8.106 | 8.060 | 0.046 |
| $Ba_2ZnWO_6$ | 8.11612 | 8.137 | -0.021 |
| $Ca_2CaWO_6$ | 8 | 8.147 | -0.147 |
| $Pb_2FeWO_6$ | 8.05 | 8.026 | 0.024 |
| $Pb_2MgTeO_6$ | 7.99 | 7.950 | 0.040 |
| $Sr_2CaOsO_6$ | 8.21 | 8.191 | 0.019 |
| $Sr_2CoUO_6$ | 8.19 | 8.149 | 0.041 |
| $Sr_2FeOsO_6$ | 7.85 | 7.895 | -0.045 |
| $Sr_2FeUO_6$ | 8.11 | 8.190 | -0.080 |
| $Sr_2MgUO_6$ | 8.19 | 8.165 | 0.025 |
| $Sr_2MnUO_6$ | 8.28 | 8.264 | 0.016 |

**Table 3** (continue) Actual, predicted values for the unit cell length, as well as, absolute errors for the compounds of the calibration set obtained by MLR.

| Formula | MLR | | | ANN | | | Ref. |
|---------|-----|---|---|-----|---|---|------|
| | $a$(act.)/Å | $a$(pred.)/Å | $|\Delta a|$/Å | $a$(act.)/Å | $a$(pred.)/Å | $|\Delta a|$/Å | |
| $Ba_2LiReO_6$ | 8.118 | 8.047 | 0.071 | 8.118 | 8.088 | 0.030 | [1] |
| $Ba_2NaReO_6$ | 8.296 | 8.327 | 0.031 | 8.296 | 8.339 | 0.043 | [1] |
| $Sr_2LiOsO_6$ | 7.860 | 7.853 | 0.007 | 7.860 | 7.868 | 0.008 | [1] |
| $Sr_2NaReO_6$ | 8.130 | 8.129 | 0.001 | 8.130 | 8.141 | 0.011 | [1] |
| $Ba_2CoReO_6$ | 8.086 | 8.006 | 0.080 | 8.086 | 8.065 | 0.021 | [1] |
| $Ba_2DyTaO_6$ | 8.545 | 8.461 | 0.084 | 8.545 | 8.446 | 0.099 | [1] |
| $Ba_2ErReO_6$ | 8.354 | 8.351 | 0.003 | 8.354 | 8.385 | 0.031 | [1] |
| $Ba_2ErUO_6$ | 8.670 | 8.650 | 0.020 | 8.670 | 8.678 | 0.008 | [1] |
| $Ba_2EuTaO_6$ | 8.506 | 8.506 | 0.000 | 8.506 | 8.497 | 0.009 | [1] |
| $Ba_2GdNbO_6$ | 8.496 | 8.495 | 0.001 | 8.496 | 8.483 | 0.013 | [1] |
| $Ba_2GdSbO_6$ | 8.440 | 8.446 | 0.006 | 8.440 | 8.424 | 0.016 | [1] |
| $Ba_2HoTaO_6$ | 8.442 | 8.449 | 0.007 | 8.442 | 8.431 | 0.011 | [1] |
| $Ba_2InPaO_6$ | 8.596 | 8.540 | 0.056 | 8.596 | 8.575 | 0.021 | [1] |
| $Ba_2InTaO_6$ | 8.280 | 8.300 | 0.020 | 8.280 | 8.278 | 0.002 | [1] |
| $Ba_2LaReO_6$ | 8.580 | 8.513 | 0.067 | 8.580 | 8.533 | 0.047 | [1] |
| $Ba_2LuTaO_6$ | 8.372 | 8.423 | 0.051 | 8.372 | 8.389 | 0.017 | [1] |
| $Ba_2NdPaO_6$ | 8.840 | 8.782 | 0.058 | 8.840 | 8.810 | 0.030 | [1] |
| $Ba_2PrPaO_6$ | 8.862 | 8.790 | 0.072 | 8.862 | 8.817 | 0.045 | [1] |
| $Ba_2ScOsO_6$ | 8.152 | 8.193 | 0.041 | 8.152 | 8.208 | 0.056 | [1] |
| $Ba_2ScSbO_6$ | 8.197 | 8.229 | 0.032 | 8.197 | 8.200 | 0.003 | [1] |
| $Ba_2SmNbO_6$ | 8.518 | 8.518 | 0.000 | 8.518 | 8.512 | 0.006 | [1] |
| $Ba_2TbPaO_6$ | 8.753 | 8.713 | 0.040 | 8.753 | 8.747 | 0.006 | [1] |
| $Ba_2TmNbO_6$ | 8.408 | 8.429 | 0.021 | 8.408 | 8.403 | 0.005 | [1] |
| $Ba_2YNbO_6$ | 8.441 | 8.453 | 0.012 | 8.441 | 8.431 | 0.010 | [3] |
| $Ba_2YTaO_6$ | 8.433 | 8.449 | 0.016 | 8.433 | 8.430 | 0.003 | [1] |
| $Ba_2YbPaO_6$ | 8.678 | 8.654 | 0.024 | 8.678 | 8.685 | 0.007 | [1] |
| $Sr_2AlNbO_6$ | 7.786 | 7.837 | 0.051 | 7.786 | 7.853 | 0.067 | [3] |
| $Sr_2CrMoO_6$ | 7.840 | 7.892 | 0.052 | 7.840 | 7.891 | 0.051 | [21] |
| $Sr_2FeBiO_6$ | 8.063 | 8.156 | 0.093 | 8.063 | 8.135 | 0.072 | [31] |
| $Sr_2InOsO_6$ | 8.060 | 8.022 | 0.038 | 8.060 | 8.012 | 0.048 | [1] |
| $Sr_2RhNbO_6$ | 7.914 | 7.926 | 0.012 | 7.914 | 7.945 | 0.031 | [24] |
| $Sr_2ScReO_6$ | 8.020 | 7.990 | 0.030 | 8.020 | 7.967 | 0.053 | [1] |
| $Ba_2BaUO_6$ | 8.890 | 9.064 | 0.174 | 8.890 | 9.002 | 0.112 | [1] |
| $Ba_2CaReO_6$ | 8.356 | 8.385 | 0.029 | 8.356 | 8.414 | 0.058 | [1] |
| $Ba_2CaWO_6$ | 8.388 | 8.462 | 0.073 | 8.388 | 8.453 | 0.065 | [26] |
| $Ba_2CdReO_6$ | 8.322 | 8.280 | 0.042 | 8.322 | 8.341 | 0.019 | [1] |
| $Ba_2CoUO_6$ | 8.374 | 8.347 | 0.027 | 8.374 | 8.343 | 0.031 | [1] |
| $Ba_2FeReO_6$ | 8.050 | 8.089 | 0.039 | 8.050 | 8.162 | 0.112 | [1] |
| $Ba_2MgOsO_6$ | 8.080 | 8.069 | 0.011 | 8.080 | 8.101 | 0.021 | [1] |

**Table 4** Actual and predicted values for the unit cell edge length, as well as, absolute errors for the compounds of the test set obtained by MLR and ANN.

| Formula | MLR | | | ANN | | | Ref. |
|---|---|---|---|---|---|---|---|
| | $a$(act.)/Å | $a$(pred.)/Å | $|\Delta a|$/Å | $a$(act.)/Å | $a$(pred.)/Å | $|\Delta a|$/Å | |
| $Ba_2MgUO_6$ | 8.381 | 8.363 | 0.018 | 8.381 | 8.336 | 0.045 | [1] |
| $Ba_2MnWO_6$ | 8.199 | 8.240 | 0.041 | 8.199 | 8.209 | 0.011 | [21] |
| $Ba_2NiReO_6$ | 8.040 | 7.987 | 0.053 | 8.040 | 8.062 | 0.022 | [1] |
| $Ba_2ZnMoO_6$ | 8.103 | 8.140 | 0.036 | 8.103 | 8.074 | 0.029 | [26] |
| $Ba_2ZnUO_6$ | 8.397 | 8.359 | 0.038 | 8.397 | 8.348 | 0.049 | [1] |
| $Ca_2MgWO_6$ | 7.700 | 7.826 | 0.126 | 7.700 | 7.819 | 0.119 | [1] |
| $Pb_2MgWO_6$ | 8.006 | 8.001 | 0.005 | 8.006 | 8.021 | 0.015 | [32] |
| $Sr_2CrUO_6$ | 8.090 | 8.224 | 0.134 | 8.090 | 8.227 | 0.137 | [1] |
| $Sr_2MgTeO_6$ | 7.940 | 7.892 | 0.048 | 7.940 | 7.894 | 0.046 | [1] |
| $Sr_2NiUO_6$ | 8.150 | 8.088 | 0.062 | 8.150 | 8.103 | 0.047 | [1] |

**Table 4** (continue) Actual and predicted values for the unit cell edge length, as well as, absolute errors for the compounds of the test set obtained by MLR and ANN.